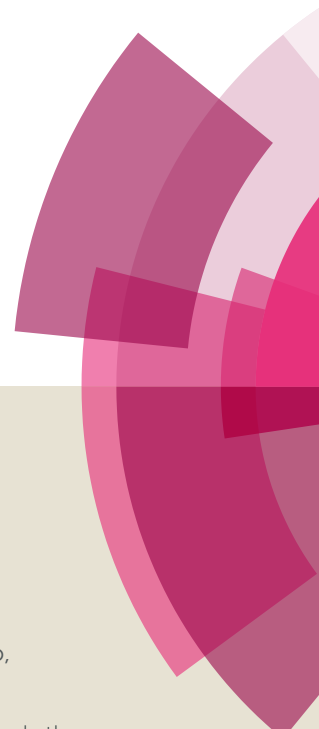


NJC

Accepted Manuscript



This article can be cited before page numbers have been issued, to do this please use: X. Peng, H. Gao, Y. Xiao, H. Cheng, F. Huang and X. Cheng, *New J. Chem.*, 2017, DOI: 10.1039/C6NJ02604D.



This is an Accepted Manuscript, which has been through the Royal Society of Chemistry peer review process and has been accepted for publication.

Accepted Manuscripts are published online shortly after acceptance, before technical editing, formatting and proof reading. Using this free service, authors can make their results available to the community, in citable form, before we publish the edited article. We will replace this Accepted Manuscript with the edited and formatted Advance Article as soon as it is available.

You can find more information about Accepted Manuscripts in the [author guidelines](#).

Please note that technical editing may introduce minor changes to the text and/or graphics, which may alter content. The journal's standard [Terms & Conditions](#) and the ethical guidelines, outlined in our [author and reviewer resource centre](#), still apply. In no event shall the Royal Society of Chemistry be held responsible for any errors or omissions in this Accepted Manuscript or any consequences arising from the use of any information it contains.

Synthesis and self-assembly of photoresponsive and luminescent polycatenar liquid crystals incorporating an azobenzene unit interconnecting two 1,3,4- thiadiazoles

Xiongwei Peng, Hongfei Gao, Yulong Xiao, Huifang Cheng, Fanran Huang, Xiaohong Cheng*

Key Laboratory of Medicinal Chemistry for Natural Resources, Chemistry Department
Yunnan University
Kunming, Yunnan 650091,
P. R. China
Fax: (+86) 871 5032905
E-mail: xhcheng@ynu.edu.cn

Abstract: Novel polycatenar liquid crystals containing two 1,3,4-thiadiazole rings interconnected by an azobenzene central linkage have been synthesized and investigated by polarizing microscopy, DSC, X-ray scattering, SEM, UV-vis spectroscopy and photoluminescence measurements. These compounds can self-assemble into SmC, Col_{hex}/*p6mm* and Cub/*Pm3n* liquid crystalline phases in the bulk states and form multistimuli responsive organogels in organic solvents. They have reversible photoresponsive properties in solution, liquid crystalline states and gel states. They also show fluorescent emission with large Stokes shift in solution and binding selectivity to Cu²⁺ among a series of cations in CH₃CN-CH₂Cl₂ solution.

Key words: 1,3,4-thiadiazole; azobenzene; luminescent liquid crystal; organogel; fluorescent chemosensor.

1. Introduction

The combination of heterocyclic rings into a liquid crystal molecule is essential to the design and synthesis of advanced functional materials. Heteroatoms like nitrogen, oxygen and sulfur provide a reduced molecular symmetry, strong lateral or longitudinal dipole and a donor–acceptor interaction within the molecule, which in turn affects the LC self-assembly and electronic behavior of the mesogens.¹ 1,3,4-Thiazole is an important five membered heterocycle which has a high aromaticity and its derivatives are applied widely in pharmaceutical, agricultural and material chemistry. With its electro-deficient nature and good electron-accepting ability as well as thermal and chemical stability, 1,3,4-thiazoles are widely applied in optics and electrochemistry focusing on their photoluminescence, photoconductivity, charge transporting capacity and mesomorphism to obtain functional liquid crystals.²

However, reports on 1,3,4-thiadiazole-based mesogens are scarce, partially due to the synthetic difficulty. Till now very few reports on 1,3,4-thiadiazole-based calamitic LCs,³ banana-shaped LCs,⁴ hydrogen-bonded LCs,⁵ polycatenar LCs,^{6,7,8} star-shaped mesogens⁹ and polymeric LCs¹⁰ etc have been reported. Compared with their 1,3,4-oxadiazole analogues, 1,3,4-thiadiazole derivatives are considered as more conducive to mesogens because of their higher melting points, clear temperatures, and viscosity, as well as efficient packing, larger dipole moments (1,3,4-thiadiazole: 3.11 D, 1,3,4-oxadiazole: 3.06 D) and their less bent molecular structures.^{1c,4a} Most of the reported 1,3,4-thiadiazole contained mesogens can self organize into nematic,^{3p, 4a}

smectic,^{3g,3h,3o} columnar phases,^{7,8,9} but no thermotropic micellar cubic phases have been reported formed by such 1,3,4-thiadiazole contained mesogens.

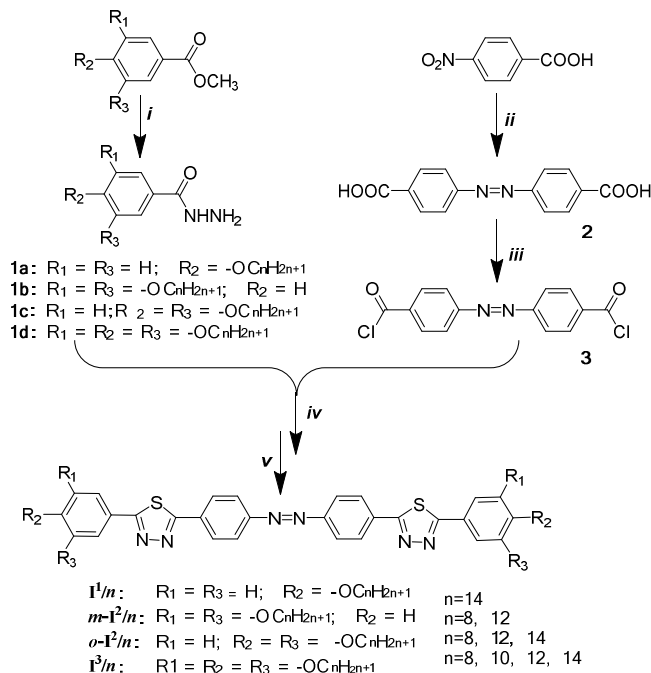
Azobenzene derivative LCs have attracted much more attention because of their photoresponsive properties caused by the *trans*–*cis* photoisomerization of the azobenzene units.¹¹ A wide diversity of azobenzene derivative LCs have been designed to introduce light-modulated functionalities, for example for application as organic light-driven actuators.^{12,13,14} Most azobenzene derivative LCs contain an azo linkage either at the periphery^{14,15,16,17,18} or in few cases also at the central of the molecules.¹⁹ The azobenzene derivatives were usually non photoluminescence (PL).²⁰ It is possible to combine azobenzene with 1,3,4-thiadiazole to design novel LCs with both photoresponsive and luminescence properties. As far as we know, such 1,3,4-thiadiazole containing polycatenar liquid crystals with an azobenzene as central links have not ever been reported.

Therefore herein we have designed and synthesized novel symmetrical polycatenar liquid crystals containing two 1,3,4-thiadiazole rings interconnected by an azobenzene central linkage, bearing alkyl chains at each terminus. These compounds are assigned as \mathbf{I}^m/n , where m stands for the number of the terminal chain at one terminus, n is the alkyl chain length. \mathbf{I}^m/n have both LC and gelation properties. Depending on the number and length of the terminal chains, different mesophase structures including smectic C, hexagonal columnar and even micellar cubic phases are found in these compounds. \mathbf{I}^m/n have photoresponsive ability in solution, LC states and gel states. \mathbf{I}^m/n can also be used as fluorescence chemosensors for selective response to Cu^{2+} among different metal ions in solution.

2. Results and Discussion

2.1. Synthesis

The synthetic route is shown in Scheme 1. Both thiadiazole rings in target compounds \mathbf{I}^m/n were formed simultaneously by reaction of azobenzene dichloride **3** with appropriate 3,4,5-trialkoxybenzhydrazides **1**²¹ and subsequent cyclization with phosphorus pentasulfide.²² Azo benzene dichloride **3** was prepared from the azobenzene-4,4-dicarboxylic acid **2** which was obtained from the reduction reaction of 4-nitrobenzoic acid with glucose under alkaline environment.²³ Purification of all the products was done by column chromatography. Experimental procedures and analytical data are collated in the Supporting Information.



Scheme 1. Synthesis of the I^m/n . *Reagents and conditions:* i) hydrazine hydrate, 2-methoxyethanol, 100 °C, 12 h; ii) NaOH, glucose, 70 °C, 12 h; iii) SOCl₂, 70 °C, 5 h; iv) Et₃N, THF, 70 °C, 12 h; v) toluene, P₂S₅, 100 °C, 12 h.

2.2. Mesomorphic properties

Table 1 Transition temperatures and associated enthalpy values (in brackets) of compounds I^l/n , $m-I^l/n$, $o-I^l/n$ and I^3/n .^[a]

Comp.	R ₁ , R ₂ , R ₃	T/°C [$\Delta H/kJ mol^{-1}$]
I^l/14	R ₁ = R ₃ = H, R ₂ = OC ₁₄ H ₂₉	Cr 131 [50.2] SmC 167 [5.6] Iso
m-I^l/8	R ₁ = R ₃ = OC ₈ H ₁₇ , R ₂ = H	Cr 67 [26.8] Iso
m-I^l/12	R ₁ = R ₃ = OC ₁₂ H ₂₅ , R ₂ = H	Cr 54 [17.9] Iso
o-I^l/8	R ₁ = H, R ₂ = R ₃ = OC ₈ H ₁₇	Cr 121 [70.8] (103[3.7] Col _{hex}) Iso
o-I^l/12	R ₁ = H, R ₂ = R ₃ = OC ₁₂ H ₂₅	Cr 85 [21.9] Col _{hex} 105 ^[b] Iso
o-I^l/14	R ₁ = H, R ₂ = R ₃ = OC ₁₄ H ₂₉	Cr 91 [39.0] Col _{hex} 119 [1.0] Iso
I³/8	R ₁ = R ₂ = R ₃ = OC ₈ H ₁₇	Cr 74 ^[b] Iso
I³/10	R ₁ = R ₂ = R ₃ = OC ₁₀ H ₂₁	Cr 68 [47.5] Iso
I³/12	R ₁ = R ₂ = R ₃ = OC ₁₂ H ₂₅	Cr ₁ 61 [10.9] Cr ₂ 70 [16.9] Cub/ <i>Pm</i> $\bar{3}n$ 80 ^[b] Iso
I³/14	R ₁ = R ₂ = R ₃ = OC ₁₄ H ₂₉	Cr ₁ 63 [11.0] Cr ₂ 67 [17.0] Cub/ <i>Pm</i> $\bar{3}n$ 82 ^[b] Iso

^[a] Transition temperatures were determined by DSC (peak temperature from the first heating scan, at a rate of 1 K min⁻¹ for **I³/8**, **I³/10**, **I³/12**, **I³/14**; 2 K min⁻¹ for compounds **I^l/14**, **m-I^l/8**, **m-I^l/12** and 5 K min⁻¹ for **o-I^l/8**, **o-I^l/12**, **o-I^l/14**). Abbreviations: Cr = crystal; SmC = smectic C phase; Col_{hex} = hexagonal columnar phase; Cub/*Pm* $\bar{3}n$ = micellar cubic mesophases with space groups *Pm* $\bar{3}n$; Iso = isotropic liquid. ^[b] Transition temperature determined by POM.

The LC self-assembly of compounds I^1/n , $m-I^2/n$, $o-I^2/n$ and I^3/n was investigated by polarized optical microscopy (POM), differential scanning calorimetry (DSC) and X-ray diffraction (XRD). The transition temperatures are shown in Table 1.

2.2.1. Dicatenaar and tetracatenar compounds (I^1/n , $m-I^2/n$, $o-I^2/n$) and their formation of smectic C and columnar hexagonal phases

Together ten compounds were prepared. They differ themselves in the number and length as well as in the substituted patterns of the alkyl chains. Dicatenaar compound $I^1/14$ with one tetradecyl chain at each terminus shows smectic C mesophase as identified by its typical SmC schlieren texture as observed under POM (Fig. S1a†).²⁴ The small-angle X-ray scattering (SAXS) pattern of this compound shows the sharp layer reflection with the thickness of $d = 5.4$ nm at 140 °C (Fig. S3a†). Comparing the diffraction peak, which corresponds to the interlayer spacing, to the molecular length $L = 6.6$ nm (estimated by Material Studio, version 6.0), one can infer that the aliphatic chains are folded or the molecules are tilted within the layers. Considering the molecules in the most extended form, the tilt angle was calculated using the relationship $\cos \theta = d/L = 0.82$ and a value of $\theta \approx 37$ degree was obtained, which is consistent with the value for the SmC phase.²⁵

Tetracatenar compounds $m-I^2/n$ ($n = 8, 12$) with two *meta*-substituted octyl and dodecyl chains respectively at each terminus are not LC. However, tetracatenar compounds with two *ortho*-substituted alkyl chains $o-I^2/n$ ($n = 8, 12, 14$) all show columnar phases, for these tetracatenar compounds, with the elongation of the alkyl chain, the melting temperatures decrease, the isotropic temperatures increase, therefore the range of mesophase broadens and the stability of mesophase increases. Compound $o-I^2/8$ is monotropic columnar mesophase, the other two higher homologues formed stable enantiotropic columnar mesophases. The columnar phases were identified by the typical spherulitic fanlike textures under POM. Investigation of the columnar phases by polarising microscopy between crossed polarisers with an additional λ -retarder plate indicates that the columnar phases of compounds $o-I^2/n$ ($n = 8, 12, 14$) are optically negative (Fig. 1b and Fig. S1b-1c†). This means that the major intramolecular π -conjugation pathway, which is along the long axis of the aromatic cores, is perpendicular to the column long axis. This is in line with the proposed organization of the molecules in the columns. The columnar phases were also investigated by SAXS. There are three small angle reflections with a ratio of their reciprocal spacing $1: 3^{1/2} : 2$, which can be indexed to the 10, 11, 20 reflections of hexagonal lattice with $p6mm$ symmetry (Fig. 1c, Fig. S4a-b† and Table S1-S3†). The number of molecules organized in a slice of the columns with a height of $h = 0.45$ nm (a typical value for the maximum of the diffuse wide angle scattering) n_{cell} could be calculated as shown in Table 2 and Table S6†. It can be assumed that for these compounds, approximately 5 molecules self-assemble into an overall disk-like stratum and they successively stack one another to form supramolecular columns, which was similar with the reported polycatenar mesogens.²⁶ It should be noted that the intermolecular π - π interactions between the azobenzene-thiadiazole cores as well as nanosegregation of the rigid aromatic center from the surrounding alkyl chain moieties would promote the assembly of these molecules into such columnar structures (Fig. 1d). Although the *meta* substituted compounds $m-I^2/8$ and $m-I^2/12$ have very low melting points, they do not show mesophases, while all the *ortho* substituted compounds are all liquid crystals. The reason is that if the two terminal alkyl chains are not close to each other, their separation into distinct defined region is disturbed and give

rise to disorder.²⁷

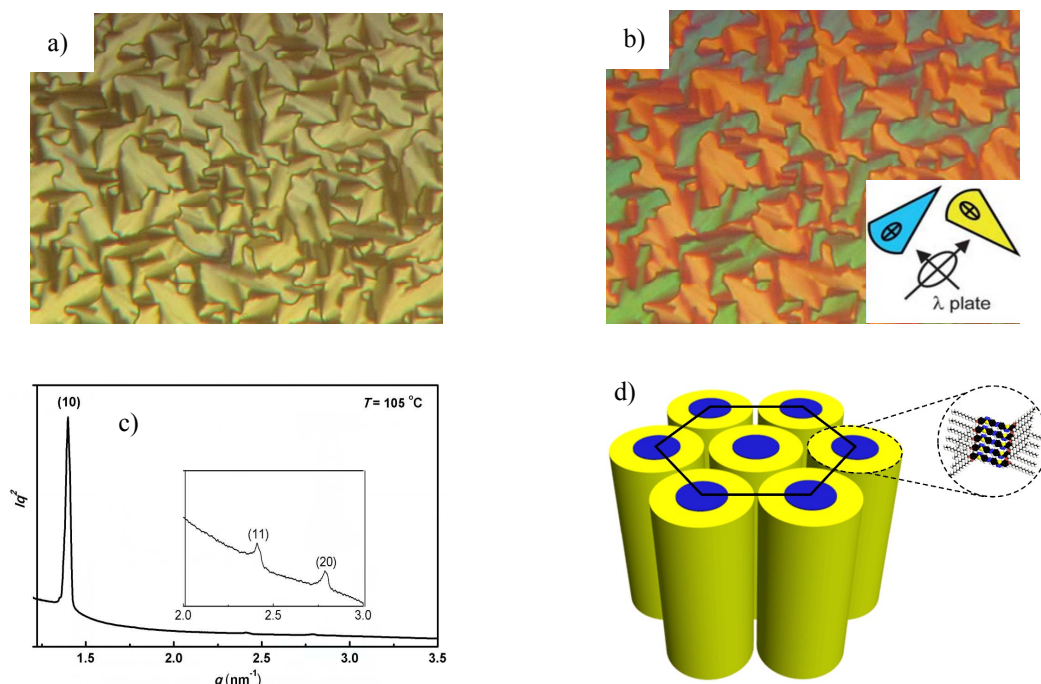


Fig. 1 Col_{hex} phase of compound *o*-I²/14: (a) texture as seen between crossed polarizers at *T* = 100 °C; (b) inset shows the same region with λ-plate; (c) SAXS diffractogram at *T* = 105 °C; (d) model showing the organization of compounds *o*-I²/*n* in Col_{hex} phase.

2.2.2. Hexacatenar compounds I³/*n* and their formation of micellar cubic phases

Interesting micellar $Pm\bar{3}n$ cubic phase is observed in hexacatenar compounds I³/12 and I³/14 with three long chains at each terminus, while the other two lower homologues (I³/8 and I³/10) are only crystals. For this cubic phase, under POM, optically isotropic texture was observed, which is not fluid, but soft and viscoelastic, by increasing the temperature, sharp transitions to highly fluid isotropic liquid occur at defined temperature (Fig. S1d-1e†). The isotropic mesophases of compound I³/14 and I³/12 were investigated by XRD, indicating the fluid LC states, and several reflections in the small-angle region that could be indexed to a cubic lattice with $Pm\bar{3}n$ space group (Fig. 2a and Fig. S3b†). The $Pm\bar{3}n$ lattice is the most commonly observed lattice of micellar cubic phases (Cub₁) occurring in thermotropic systems formed by spheroidal aggregates with soft corona.²⁸ Hence, it is highly reasonable to illustrate that the LC phases of the compound I³/12 and I³/14 represent $Pm\bar{3}n$ micellar cubic phases. This is in line with the position of these cubic phases in the quence SmC–Col_{hex}–Cub₁ as observed upon increasing the number and length of the aliphatic chains. By calculation, each micelle is built up of approximately 28 and 27 molecules in the $Pm\bar{3}n$ cubic phase of I³/12 and I³/14 respectively (Table 2 and Table S6†). The π -conjugated azobenzene-thiadiazole moieties occupy the core encapsulated by the alkyl chain moieties in the micelles (Fig. 2b). By comparison with the reported azo free hexacatenar analogues I³/*n*,⁷ which can display only columnar phases (Fig. 3), the incorporation of azobenzene unit into the thiadiazole contained rigid cores of polycatenar compounds, enhanced the formation of Cub₁ phase. The large volume of the flexible chain and the extended twist-bend

azobenzene core should enhance the nanosegregation between the flexible tails and the extended rigid cores and give rise to a large interface curvature, thus contribute to the emergence of the cubic phase. The extended twist-bend azobenzene core and possible *trans-cis* transformation of central azobenzene unit could contribute to the formation of the softness of these spheres in cubic phase, and this is favorable for the organization in a $Pm\bar{3}n$ lattice instead of other cubic phases.

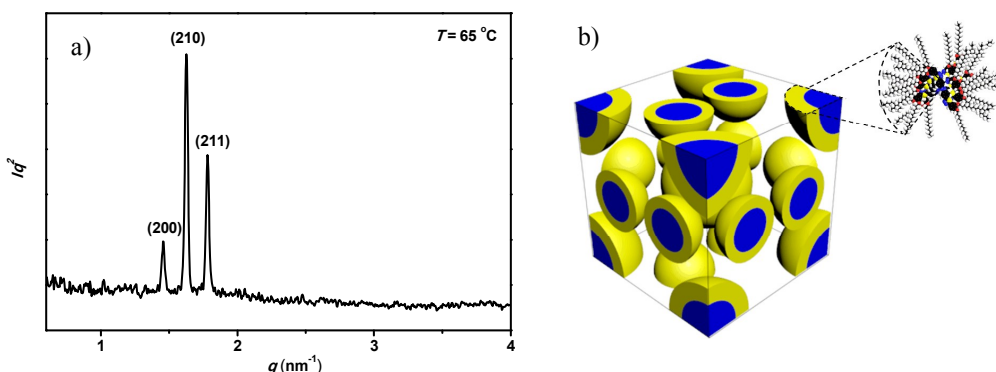


Fig. 2 (a) SAXS diffractograms of compound $I^3/14$; (b) possible molecular organization in $Pm\bar{3}n$ micellar cubic phase.

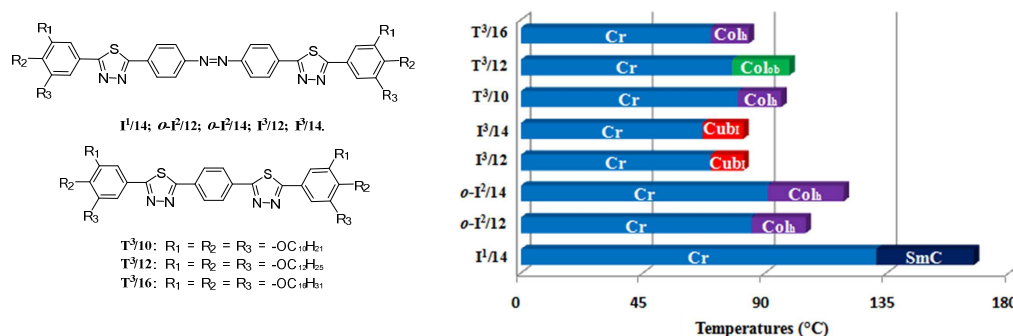


Fig. 3 Bar graph summarizing the thermal behavior of researched compounds I^3/n and the reported compounds T^3/n .

Table 2 Comparison of X-ray data and molecular dimensions of the columnar and cubic phases^[a]

Comp.	Phase, Plane/space group	L [nm]	a [nm] (T [°C])	n
$o-I^2/8$	$Col_{hex}/p6mm$	5.82	4.80 (100)	4.8
$o-I^2/12$	$Col_{hex}/p6mm$	6.32	5.28 (90)	5.2
$o-I^2/14$	$Col_{hex}/p6mm$	6.58	5.20 (105)	4.7
$I^3/12$	$Cub/Pm\bar{3}n$	6.32	8.46 (70)	28
$I^3/14$	$Cub/Pm\bar{3}n$	6.58	8.65 (65)	27

^[a] Abbreviations: a = lattice parameter determined by XRD (a_{hex} and a_{cub} , respectively); L = molecular length of a molecule measured between the ends of the terminal chains and assuming a most stretched conformation with all-*trans* conformation of the alkyl chains; n = number of molecules in the cross section of a column in the Col_{hex} phases (with assumed height of 0.45 nm) or number of molecules in each aggregate of the $Cub/Pm\bar{3}n$ lattice. For Col_{hex} phase: $n = (a^2/2)\sqrt{3}h(N_A/M)\rho$, N_A = Avogadro constant, M = molecular mass, assuming a density of $\rho = 1$

g/cm^3 ; for $\text{Cub}_I/Pm\bar{3}n$ phase: $n = n_{\text{cell}}/8$.

In all cases shearing the samples led to flow which removes the textures, this confirms the LC states of these materials. With increasing the number of alkyl chains, namely increasing the fraction of the alkyl chains, the interface curvature between the nanosegregated regions of the azobenzene-thiadiazole cores and the flexible chains should be increased. This structural variation gives rise to the transition from the SmC through hexagonal columnar (Col_{hex}) to cubic ($\text{Cub}_I/Pm\bar{3}n$) LC phases, which is similar to the mesomorphism of amphiphiles and block molecules.²⁹

2.3. Photoisomerization behavior in liquid crystalline and solution

The effect of *trans*-to-*cis* photoisomerization caused by the UV irradiation on the thermotropic LC phases of these compounds was investigated. All the liquid crystalline phases can respond to the UV irradiation immediately by changing their textures to isotropic state and recovering to their LC textures after removing the UV source. This means that all the compounds showed *trans* to *cis* photoisomerization under UV irradiation and *cis* to *trans* thermal isomerization under visible light irradiation. For example, sample **I¹/14** was cooled from the isotropic liquid state to 145 °C in the range of the SmC phase (Fig. 4a). After annealing for 5 minutes, the sample was exposed to UV irradiation at 365 nm (10 mW cm^{-2}) for 1 second, the schlieren texture of the SmC phase is disappeared and replaced by isotropic one (Fig 4a-b). After removal of the UV lamp, the schlieren texture of the SmC phase renewed (Fig. 4b-c). It seems that the *trans*-to-*cis* photoisomerization effect on the liquid crystalline property of the compounds reported here is very strong. Schematic illustration of the photochemical switching possible process of SmC–Iso reversible transition of **I¹/14** is shown in Fig. 5. Similarly, the compound **o-I²/14** showed photoisomerization reversible transition of Col –Iso (Fig. S5†). Such photoisomerizations could be useful for light sensitive displays or data storage applications.^{19a,30}

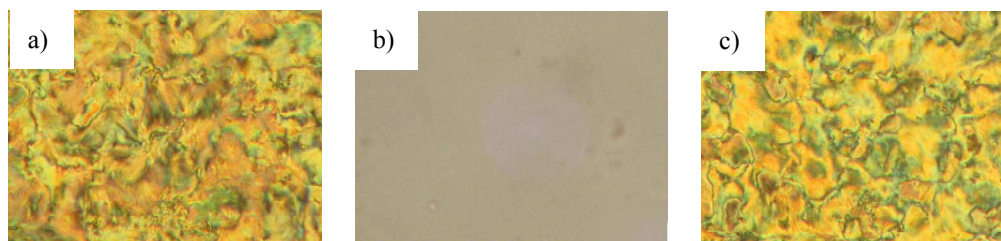


Fig. 4 Textural changes as observed by POM at the photoinduced SmC-Iso transition and the relaxation Iso-SmC as observed for compound **I¹/14** at 145 °C: (a) before UV irradiation; (b) after UV irradiation for 1 s; (c) after visible light irradiation for 1 s.

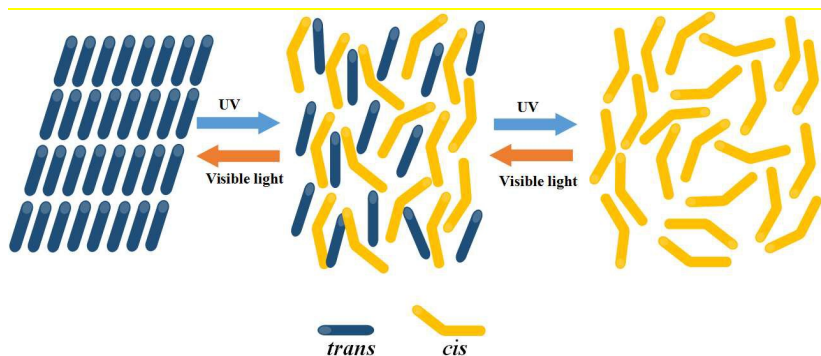


Fig. 5 Schematic illustration of the photochemical switching possible process in $I^1/14$; (a) SmC phase; (b) SmC–Iso transition; (c) isotropic phase.

Such compounds exhibit the expected reversible *trans*-to-*cis* photoresponsive behavior in solution (Fig. S6-8†).

2.4. Absorption and emission properties

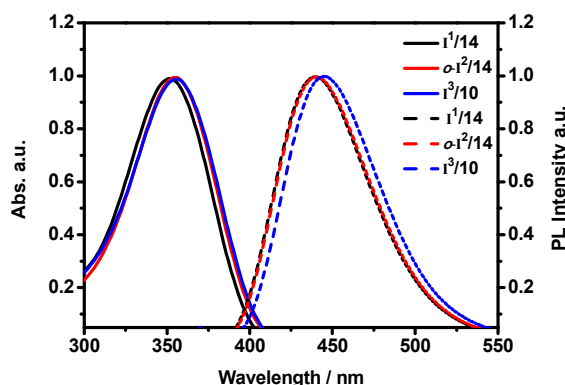


Fig. 6 Normalized absorption (solid line) and emission spectra (dotted line) in THF solution obtained for $I^1/14$, $o-I^2/14$ and $I^3/10$.

The UV-vis absorption and fluorescence spectroscopic data of the chosen representative compounds $I^1/14$, $o-I^2/14$, $I^3/10$ in THF solution ($c = 10^{-6}$ mol L $^{-1}$) are shown in Fig. 6. These compounds show the maximum absorption peak at about 355 nm and maximum emission peak range of 440–450 nm in THF solution which may be attributed to the π - π^* transition. It is surprised to see that compounds $I^1/14$, $o-I^2/14$, $I^3/10$ have a large Stokes shift of 101 nm, 100 nm and 103 nm, respectively. Compared to their polycatenar analogue $T^3/10$ (absorption maximum at 365 nm),⁷ compounds $I^3/10$ shows hypsochromic shift for 10 nm in the absorption maximum (355 nm) (Table S7†), indicating that the enhanced molecular transmittance (i.e. blue-shift of λ_{\max}) is mainly due to the azobenzene conjugate bridge structures in chromophores.^{31,32} The UV-vis absorption spectrum of compound $I^3/14$ in the solid state exhibits a blue-shifted absorption with maximum at 352 nm, while its solution displays a structured absorption with a maximum at 363 nm. The blue-shifted in solid state suggests the formation of π -stacked aggregates with a *H*-type parallel stacking mode in the solid state (Fig. S9†).³³

The energy band gap of compound $I^3/14$, which was estimated from the onset of the

absorption in film, is about 2.5 eV (Fig. S10†).³⁴ In order to investigate the conformation and electron distributions of **I¹/14**, ***o*-I²/14**, **I³/10**, calculations based on density functional theory (DFT) with the Gaussian 03 W program package at B3LYP/(6-31G, d) level were performed with the model compounds **I¹/14**, ***o*-I²/14**, **I³/10**. The electron distributions of the HOMO and LUMO of **I¹/14**, ***o*-I²/14**, **I³/10** are shown in Fig. S11†. In the minimum energy conformation, compounds **I¹/14**, ***o*-I²/14**, **I³/10** adopt almost a bar shaped conformation with kinks provided by the azobenzene groups, linking the peripheral phenyl groups to the 1,3,4-thiadiazole. As it can be seen in the HOMO orbital, the electrons are localized on the thiadiazole unit of the central-conjugated azobenzene core. In the LUMO orbital, the electrons are mainly localized on the azobenzene-thiadiazole unit, indicating that intramolecular charge transfer (ICT) might exist in these molecules. The band-gap of the HOMO and LUMO energy levels of **I³/14** (Fig. S11†) was almost in agreement with those obtained from their absorption spectra in film.

2.5. Gelation properties

Among the synthesized polycatenar compounds **I^m/n**, only hexacatenar compounds **I³/n** have the gelation abilities. The gelation ability of the representative compound **I³/10** was tested in various organic solvents at a concentration of 6.0 mg/mL and the results are summarized in Table 3. **I³/10** has the ability to gel in ethanol. A yellow gel can be obtained by cooling the heated solution of **I³/10** in ethanol quickly below 20 °C or slowly down to room temperature (Fig. 7c). So far as we known, there is no report about the gelation behavior of thiadiazole contained polycatenar compounds.⁷ Our study has shown that the incorporation of azobenzene with thiadiazole heterocycle induced the formation of luminescent gel of compound **I³/10**. π - π Interactions as well as van der Waals forces may play an important role for the aggregation of the compounds in solvents as exist in many azobenzene based gelators.³⁵ Under irradiation with 365 nm light the luminescent gel can be obtained (Fig. 7d). The organogels exhibit multiple stimuli-responsive behavior namely gel-sol reversible trans process upon exposure to a number of environmental stimuli including light, temperature, and shear, etc (Fig. 8). Irradiation with UV light, application of heat or shear resulted in a sol state through disruption of the non-covalent interactions between the molecules, the gel state can be recovered by the removal of such stimuli. Such multiple stimuli-responsive behaviors could be useful for drug controlled release,³⁶ energy transfer,³⁷ hardeners of solvents and sensors etc.³⁸ In order to obtain a visual insight into the morphologies of the molecular aggregation model, the gel was investigated by scanning electron microscopy (SEM). The SEM image of the xerogel formed by **I³/10** (Fig. S12†) shows the formation of three-dimensional networks composed of entangled fibrous aggregates. The approximate diameter of the fibers is 80-90 nm. The length is more than 25 μ m. On the basis of this result, it is assumed that compound **I³/10** forms fibrous aggregate in the solvent.

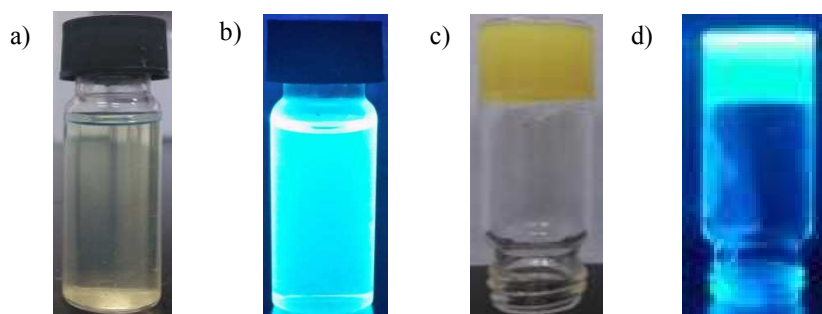


Fig. 7 Photograph of solution and gels prepared with $I^3/10$ in ethanol, 10^{-6} M, $T = 20$ °C. (a) without irradiation; (b) under irradiation with 365 nm light; (c) without irradiation and (d) under irradiation with 365 nm light.

Table 3 Gelation properties of $I^3/10$ ^[a]

Solvent	I	Solvent	I
CHCl ₃	S	CH ₂ Cl ₂	S
Ethyl acetate	S	Cyclohexane	S
Hexane	P	Ethanol	G
Methanol	PG	<i>n</i> -Butanol	S
Acetone	P	Toluene	S
DMF	P	THF	S

^[a] S = solution, P = precipitation, G = gelation, PG = partial gelation, gels formed at room temperature (20 °C).

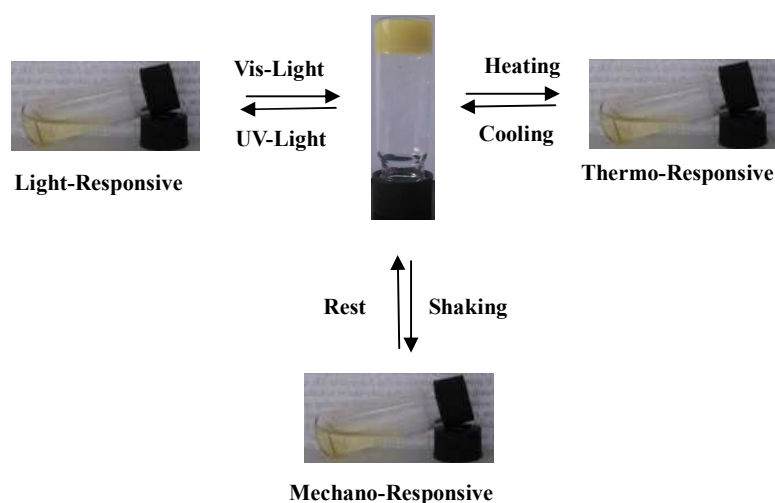


Fig. 8 Multistimuli responsive organogels formed by compound $I^3/10$ in ethanol (6.0 mg/mL).

2.6. Chemosensor behavior

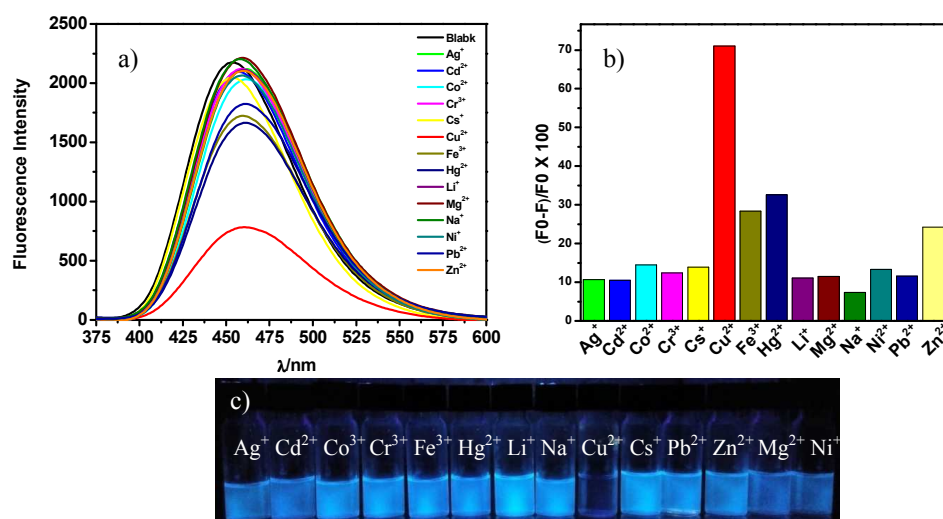


Fig. 9 Fluorescence spectra of compound ***o*-I²/14** (10^{-6} M) at room temperature, all anions are ClO_4^- , at pH = 7.0. (a) $\text{CH}_2\text{Cl}_2 : \text{CH}_3\text{CN} = 2 : 1$ ($\lambda_{\text{ex}} = 352$ nm); $(F_0-F)/F_0 \times 100$ depicts the cation selective fluorescence quenching efficiency of compound ***o*-I²/14** namely the fluorescence responses of different metal ions; abbreviation: F_0 = the fluorescence emission maximum of blank sample; F = the fluorescence emission maximum of samples with addition of different metal ions; (c) the samples with addition of different metal ions, under irradiation with 365 nm light.

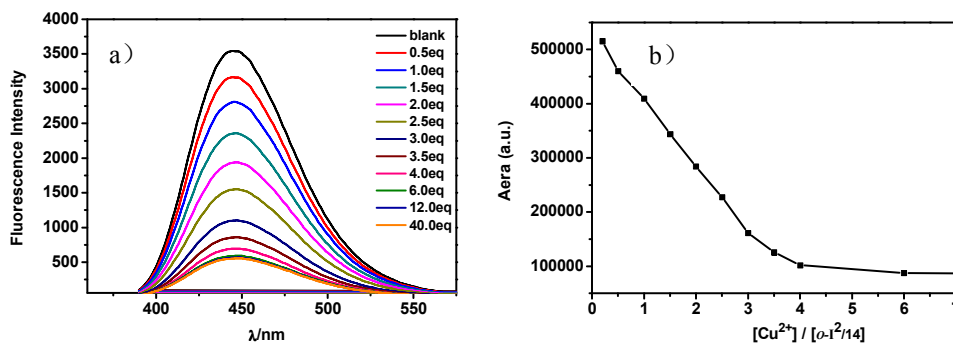


Fig. 10 (a, b) Fluorescence spectra of compound ***o*-I²/14** (1×10^{-5} M) at 20 °C upon addition of Cu^{2+} (from 0.5 to 40.0 equiv) in $\text{CH}_2\text{Cl}_2 : \text{CH}_3\text{CN} = 2 : 1$ ($\lambda_{\text{ex}} = 360$ nm).

To get insights into the binding properties of compounds ***I^m/n*** toward metal ions, the selectivity of compounds ***I^m/n*** for metal ions was examined by monitoring the change of fluorescence intensity upon the addition of various metal ions, including Ag^+ , Cd^{2+} , Cr^{3+} , Fe^{3+} , Hg^{2+} , Li^+ , Na^+ , Cu^{2+} , Cs^+ , Pb^{2+} , Zn^{2+} , Mg^{2+} , Ni^+ , Co^{3+} , the concentration of all metal ions is 10^{-3} mol L^{-1} . Compounds ***I^m/n*** all showed good selectivity for Cu^{2+} . The result of the representative compound ***o*-I²/14** is shown in Fig. 9. It was found that the fluorescence intensity of the compound ***o*-I²/14** changed little in the presence of most metal ions examined, except Cu^{2+} . The obvious fluorescence quenching was observed upon only increasing addition of Cu^{2+} . As is evident from Fig. 9a-c, indicating that ***o*-I²/14** has a high and single selectivity, and can serve as a potential chemosensor for detection of Cu^{2+} in $\text{CH}_2\text{Cl}_2 : \text{CH}_3\text{CN}$. Till now there are only few reports on 1,3,4-thiadiazole derivatives serving as a potential chemosensor for detection of Cu^{2+} by “naked-eye”.^{39,40}

For the selective response of ***o*-I²/14** to Cu^{2+} , spectral titration was performed in solution of $\text{CH}_2\text{Cl}_2 : \text{CH}_3\text{CN} = 2 : 1$; with the addition of Cu^{2+} (from 0.5 to 40 equiv), the emission peak at 452 nm decreased gradually and finally reached its fluorescence quenching plateau at ~ 6 equiv (Fig. 10a-b).⁴¹ Therefore, compound ***o*-I²/14** could be used as chemosensor exhibiting strong and selective binding to Cu^{2+} in the solution of $\text{CH}_2\text{Cl}_2 : \text{CH}_3\text{CN} = 2 : 1$. Cu^{2+} is a significant environmental pollutant due to its widespread use. The development of chemosensors for the detection and monitoring of Cu^{2+} , with high sensitivity, low detection limit and quick response, is in a great demand.⁴²

3. Conclusion

Series of polycatenar liquid crystals containing two 1,3,4-thiadiazole rings interconnected by an azobenzene central link have been synthesized. The incorporation of azobenzene with thiadiazole into the rigid core produced a new kind of photoresponsive and fluorescence polycatenar liquid

crystals. With increasing the number and length of the terminal alkyl chains, not only smectic C phase and hexagonal columnar phase, but also micellar cubic ($Cub_I/Pm\bar{3}n$) phase are found in these compounds. The formation of the micellar cubic phase is due to the larger interface curvature between the flexible chains and rigid core. The extended twist bent azobenzene core is flexible in some degree and lead to the formation of $Pm\bar{3}n$ cubic phase instead of other cubic structures. The reversible photoresponsive behavior of these compounds in liquid crystalline, solution states and gel states were well demonstrated. They also exhibit a lower band gap offering great potential in organic light emitting diode applications and shows fluorescent emission with large Stokes shift in solution and have binding selectivity to Cu^{2+} among a series of cations in $CH_3CN-CH_2Cl_2$ solution. Such multifunctional materials should have great potentials in displays, photochemical molecular switches, chemosensor etc.

Experimental

The detailed synthetic procedures, purification of the compounds together with the analytical data are reported in the Supporting Information. Tetrahydrofuran (THF) was distilled from sodium prior to use. Toluene and triethylamine was distilled from calcium hydride prior to use. Commercially available chemicals were used as received. 1H NMR and ^{13}C NMR spectra were recorded in $CDCl_3$ solution on a Bruker-DRX-400 spectrometer with tetramethylsilane (TMS) as the internal standard. Elemental analysis was performed using an Elemental VARIO EL elemental analyzer. Column chromatography was performed with silica gel 60 (230-400 mesh) from Merck. A Mettler heating stage (FP 82 HT) was used for polarizing optical microscopy (POM, Optiphot 2, Nikon) and DSC were recorded with a DSC 200 F3 Maia calorimeter (NETZSCH) at $5 K min^{-1}$. UV-vis absorption spectra were recorded on a UV-240 UV-visible spectrophotometer (Shimadzu, Japan). Fluorescence spectra were recorded using a Hitachi F-7000 fluorescence spectrometer (Hitachi, Japan). SEM experiments were carried out on a QUNT200 scanning electron microscopy (SEM, USA). All pictures were taken digitally. For the sample preparation, the gel was placed on an aluminium foil for some time until the gel became dry gel. Then gold plating, finally put the sample into the scanning electron microscopy for observation.

The small-angle X-ray diffraction measurements were also performed in transmission mode with synchrotron radiation at the 1W2A SAXS beam line at Beijing Accelerator Laboratory and Shanghai Synchrotron Radiation Facility.

Acknowledgements

This work was supported by the National Natural Science Foundation of China [no. 21364017, no. 21274119, 21274132], the Yunnan Natural Science Foundation [no. 2013FA007] and Yunnan Provincial Department of Education Foundation [no. ZD2015001] and Yunnan University Graduate Research and Innovation Foundation Project (no. YNUY201682). The calculations were performed with the support of the Yunnan University Supercomputer Center.

References

- (a) V. V. Titov and A. I. Pavlyuchenko, *Chem. Heterocycl. Compd.*, 1980, **16**, 1–13; (b) M. P. Aldred, P. Vlachos, D. Dong, S. P. Kitney, W. C. Tsoi, M. O. Neill and S. M. Kelly, *Liq. Cryst.*, 2005, **32**, 951–965; (c) A. Seed, *Chem. Soc. Rev.*, 2007, **36**, 2046–2069; (d) B. Roy, N. De and K. C. Majumdar, *Chem. Eur. J.*, 2012,

- 18, 14560–14588; (e) J. Han, *J. Mater. Chem. C.*, 2013, **1**, 7779–7797.
- 2 Y. Hu, C.Y. Li, X. M. Wang, Y. H. Yang and H. L. Zhu, *Chem. Rev.*, 2014, **114**, 5572–5610.
- 3 (a) M. Parra, S. Hernandez, J. Alderete and C. Zuniga, *Liq. Cryst.*, 2000, **27**, 995–1000; (b) Y. Xu, W. Lu and Z. Tai, *Mol. Cryst. Liq. Cryst. Sci. Technol., Sect. A*, 2000, **350**, 151–159; (c) A. A. Kiryanov, P. Sampson and A. J. Seed, *J. Org. Chem.*, 2001, **66**, 7925–7929; (d) M. W. Schroder, S. Diele, G. Pelzl, N. Pancenko and W. Weissflog, *Liq. Cryst.*, 2002, **29**, 1039–1046; (e) M. Parra, J. Alderete and C. Zuniga, *Liq. Cryst.*, 2004, **31**, 1531–1537; (f) M. Parra, J. Vergara, P. Hidalgo, J. Barbera and T. Sierra, *Liq. Cryst.*, 2006, **33**, 739–745; (g) B. P. Sybo, A. Bradley, S. Grubb, K. Miller, J. W. Proctor, L. Clowes, M. R. Lawrie, P. Sampson and A. J. Seed, *J. Mater. Chem.*, 2007, **17**, 3406–3411; (h) M. Parra, S. Villouta, V. Vera, J. Belmar, C. Zuniga and H. Z. Zunza, *Z. Naturforsch., B: J. Chem. Sci.*, 1997, **52**, 1533–1538; (i) J. Han, X. Y. Chang, L. R. Zhu, Y. M. Wang, J. B. Meng, S. W. Lai and S. S. Y. Chui, *Liq. Cryst.*, 2008, **35**, 1379–1394; (j) J. H. Tomma, I. H. Rou'il and A. H. Al-Dujaili, *Mol. Cryst. Liq. Cryst.*, 2009, **501**, 3–19; (k) M. C. McCairn, T. Kreouzis and M. L. Turner, *J. Mater. Chem.*, 2010, **20**, 1999–2006; (l) A. K. Prajapati and V. Modi, *Liq. Cryst.*, 2011, **38**, 191–199; (m) Q. Song, D. Nonnenmacher, F. Giesselmann and R. P. Lemieux, *J. Mater. Chem. C*, 2012, **1**, 343–350; (n) P. Tuzimoto, D. M. P. O. Santos, T. D. S. Moreira, R. Cristiano, I. H. Bechtold and H. Gallardo, *Liq. Cryst.*, 2014, **41**, 1097–1108; (o) R. C. Tandel and N. K. Patel, *Liq. Cryst.*, 2014, **41**, 495–502.
- 4 (a) M. Lehmann, J. Seltmann, A. Auer, E. Prochnow and U. Benedikt, *J. Mater. Chem.*, 2009, **19**, 1978–1988; (b) M. Lehmann and J. Seltmann, *Beilstein J. Org. Chem.*, 2009, **5**, 73.
- 5 M. L. Parra, E. Y. Elgueta, J. A. Ulloa, J. M. Vergara and A. I. Sanchez, *Liq. Cryst.*, 2012, **39**, 917–925.
- 6 C. F. He, G. J. Richards, S. M. Kelly, A. E. A. Contoret and M. O'Neill, *Liq. Cryst.*, 2007, **34**, 1249–1267.
- 7 S. K. Pathak, S. Nath, R. K. Gupta, D. S. S. Rao, S. K. Prasad and A. S. Achalkumar, *J. Mater. Chem. C.*, 2015, **3**, 8166–8182.
- 8 K. T. Lin, H. M. Kuo, H. S. Sheu and C. K. Lai, *Tetrahedron.*, 2013, **69**, 9045–9055.
- 9 (a) K. S. Mustafa, K. S. Al-Malki, A. S. Hameed and A. H. Al-Dujaili, *Mol. Cryst. Liq. Cryst.*, 2014, **593**, 34–42; (b) F. A. Olate, J. A. Ulloa, J. M. Vergara, S. A. Sánchez, J. Barberá and M. L. Parr, *Liq. Cryst.*, 2014, **43**, 811–827; (c) S. K. Pathak, R. K. Gupta, S. Nath, D. S. Shankar Rao, S. K. Prasad and A. S. Achalkumar, *J. Mater. Chem. C.*, 2015, **3**, 2940–2952.
- 10 (a) M. Sato, *Macromol. Rapid Commun.*, 1999, **20**, 77–80; (b) M. Sato and Y. Uemoto, *Macromol. Rapid Commun.*, 2000, **21**, 1220–1225; (c) M. Sato, M. Notsu, S. Nakashima and Y. Uemoto, *Macromol. Rapid Commun.*, 2001, **22**, 681–686; (d) M. Sato, M. Mizoi and Y. Uemoto, *Macromol. Chem. Phys.*, 2001, **202**, 3634–3641; (e) M. Sato, S. Nakashima and Y. Uemoto, *J. Polym. Sci., Part A: Polym. Chem.*, 2003, **41**, 2676–2687; (f) N. S. Al-Muaikel, *Polym. Int.*, 2004, **53**, 301–306; (g) M. Sato, Y. Tada, S. Nakashima, K.-I. Ishikura, M. Handa and K. Kasuga, *J. Polym. Sci., Part A: Polym. Chem.*, 2005, **43**, 1511–1525; (h) M. Sato, Y. Matsuoka and I. Yamaguchi, *Liq. Cryst.*, 2012, **39**, 1071–1081.
- 11 (a) T. Ube and T. Ikeda, *Angew. Chem., Int. Ed.*, 2014, **53**, 10290–10299; (b) H. M. D. Bandarab and S. C. Burdette, *Chem. Soc. Rev.*, 2012, **41**, 1809–1825; (c) J. H. Sung, S. Hirano, O. Tsutsumi, A. Kanazawa, T. Shiono and T. Ikeda, *Chem. Mater.*, 2002, **14**, 385–391.
- 12 (a) T. Ikeda, J. Mamiya and Y. Yu, *Angew. Chem., Int. Ed.*, 2007, **46**, 506–528; (b) E. V. Fleischmann and R. Zentel, *Angew. Chem., Int. Ed.*, 2013, **52**, 8810–8827; (c) Y. Yu, M. Nakano and T. Ikeda, *Nature*, 2003, **425**, 145; (d) Y. Yu, M. Nakano, A. Shishido, T. Shishido and T. Ikeda, *Chem. Mater.*, 2004, **16**, 1637–1643; (e) M. Kondo, Y. Yu and T. Ikeda, *Angew. Chem., Int. Ed.*, 2006, **45**, 1378–1382; (f) Y. Yu, T. Maeda, J. Mamiya and T. Ikeda, *Angew. Chem., Int. Ed.*, 2007, **46**, 881–883; (g) Y. Zhang, J. Xu, F. Cheng, R. Yin, C. C. Yen and Y. Yu, *J. Mater. Chem.*, 2010, **20**, 7123–7130.
- 13 (a) T. Ikeda, T. Sasaki and K. Ichimura, *Nature*, 1993, **361**, 428–430; (b) T. Sasaki, T. Ikeda and K. Ichimura,

- J. Am. Chem. Soc.*, 1994, **116**, 625–628; (c) H. J. Coles, H. G. Walton, D. Guillon and G. Poetti, *Liq. Cryst.*, 1993, **15**, 551–558; (d) A. Langhoff and F. Giesselmann, *Ferroelectrics*, 2000, **244**, 283–293.
- 14 N. G. Nagaveni, M. Gupta, A. Roy and V. Prasad, *J. Mater. Chem.*, 2010, **20**, 9089–9099.
- 15 M. L. Rahman, C. Tschierske, M. Yusoff and S. Silong, *Tetrahedron Lett.*, 2005, **46**, 2303–2306.
- 16 H. Adachi, Y. Hirai, T. Ikeda, M. Maeda, R. Hori, S. Kutsumizu and T. Haino, *Org. Lett.*, 2016, **18**, 924–927.
- 17 S. Yagai, M. Yamauchi, A. Kobayashi, T. Karatsu, A. Kitamura, T. Ohba and Y. Kikkawa, *J. Am. Chem. Soc.*, 2012, **134**, 18205–18208.
- 18 (a) S. Yagai, T. Nakajima, K. Kishikawa, S. Kohmoto, T. Karatsu and A. Kitamura, *J. Am. Chem. Soc.*, 2005, **127**, 11134–11139; (b) M. Alaasar, *Liq. Cryst.*, 2016, **43**, 1–36.
- 19 (a) E. Westphal, I. H. Bechtold and H. Gallardo, *Macromolecules.*, 2010, **43**, 1319–1328; (b) M. Cigl, A. Bubnov, M. Kašpar, F. Hampl, V. Hamplová, O. Pacheroová and J. Svoboda, *J. Mater. Chem. C.*, 2016, **4**, 5326–5333; (c) N. G. Nagaveni, P. Raghuvanshi, A. Roy and V. Prasad, *Liq. Cryst.*, 2013, **40**, 1238–1254.
- 20 H. Rau, *Angew. Chem., Int. Ed.*, 1973, **12**, 224–235.
- 21 (a) J. C. Tang, R. Huang, H. F. Gao, X. H. Cheng, M. Prehm and C. Tschierske, *RSC Adv.*, 2012, **2**, 2842–2847; (b) X. Y. Yang, H. Dai, Q. Y. He, J. C. Tang, X. H. Cheng, M. Prehm and C. Tschierske, *Liq. Cryst.*, 2013, **40**, 1028–1034.
- 22 K. Dimitrowa, J. Hauschild, H. Zaszke and H. Schubert, *J. Prakt. Chem.*, 1980, **322**, 933–944.
- 23 L. H. He, G. M. Wang, Q. Tang, X. K. Fu and C. B. Gong, *J. Mater. Chem. C.*, 2014, **2**, 8162–8169.
- 24 I. Dierking, *Textures of Liquid Crystals.*, Wiley-VCH, Weinheim, 2003.
- 25 (a) E. Giroto, I. H. Bechtold and H. Gallardo, *Liquid Crystals.*, (2016) DOI:10.1080/02678292.2016.1201159; (b) S. Q. Qu, X. F. Chen, X. Shao, F. Li, H. Y. Zhang, H. Wang, P. Zhang, Z. X. Yu, K. Wu, Y. Wang and M. Li, *J. Mater. Chem.*, 2008, **18**, 3954–3964.
- 26 (a) H. T. Nguyen, C. Destrade and J. Malthête, *Adv. Mater.*, 1997, **9**, 375–378; (b) D. Fazio, C. Mongin, B. Donnio, Y. Galerne, D. Guillon and D. W. Bruce, *J. Mater. Chem.*, 2001, **11**, 2852–2863.
- 27 M. Gharbia, A. Gharbi, H. T. Nguyen and J. Malthete, *Current Opinion in Colloid and Interface Science.*, 2002, **7**, 312–325.
- 28 (a) G. Ungar and X. Zeng, *Soft Mater.* 2005, **1**, 95–106; (b) P. Ziherl and R. D. Kamien, *J. Phys. Chem. B.*, 2001, **105**, 10147–10158.
- 29 (a) *Handbook of Liquid Crystals* (Eds: D. Demus, J. W. Goodby, G. W. Gray, H.-W. Spiess and V. Vill), Wiley-VCH, Weinheim, 1998; (b) C. Tschierske, *J. Mater. Chem.*, 2001, **11**, 2647–2671.
- 30 X. P. Tan, Z. Li, M. Xia and X. H. Cheng, *RSC Adv.*, 2016, **6**, 20021–20026.
- 31 X. Tang, L. Pan, K. Jia and X. Z. Tang, *Chem. Phys. Lett.*, 2016, **648**, 114–118.
- 32 X. Tang, K. Jia, X. Z. Tang, L. Chen and L. Pan, *J. Mater. Sci.*, 2016, **27**, 7174–7182.
- 33 (a) T. Yasuda, K. Kishimoto and T. Kato, *Chem. Comm.*, 2006, **32**, 3399–3401; (b) F. Würthner, C. Thalacker, S. Diele and C. Tschierske, *Chem. Eur. J.*, 2001, **7**, 2245–2253.
- 34 R. S. Dariani and R. Zafari, *J. Optoelectron. Adv. Mater.*, 2014, **16**, 1351–1355.
- 35 S. S. Babu, V. K. Praveen and A. Ajayaghosh, *Chem. Rev.*, 2014, **114**, 1973–2129.
- 36 A. Friggeri, B. L. Feringa and J. van Esch, *J. Controlled Release.*, 2004, **97**, 241–248.
- 37 V. K. Praveen, S. J. George, R. Varghese, C. Vijayakumar and A. Ajayaghosh, *J. Am. Chem. Soc.*, 2006, **128**, 7542–7550.
- 38 R. M. Yang, S. H. Peng and T. C. Hughes, *Soft Matter*, 2014, **10**, 2188–2196.
- 39 G. R. You, G. J. Park, J. J. Lee and C. Kim, *Dalton Trans.*, 2015, **44**, 9120–9129.
- 40 K. R. Bandi, A. K. Singh and A. Upadhyay, *Mater. Sci. Eng. C.*, 2014, **34**, 149–157.
- 41 X. P. He, Z. Song, Z. Z. Wang, X. X. Shi, K. Chen and G. R. Chen, *Tetrahedron*, 2011, **67**, 3343–3347.

42 R. Krämer, *Angew. Chem., Int. Ed.*, 1998, **37**, 772–773.

Graphical Abstract

Synthesis and self-assembly of photoresponsive and luminescent polycatenar liquid crystals incorporating an azobenzene unit interconnecting two 1,3,4- thiadiazoles

Xiongwei Peng, Hongfei Gao, Yulong Xiao, Huifang Cheng, Fanran Huang, Xiaohong Cheng*

Key Laboratory of Medicinal Chemistry for Natural Resources, Chemistry department, Yunnan University, Kunming 650091, P. R. China



Target compounds can self-assemble into thermotropic LC phase sequence of SmC-Col_{hex}-Cub₁, and have binding selectivity to Cu²⁺.